Geophysical Research Letters

RESEARCH LETTER
10.1029/2020GL087770

Special Section:
The Arctic: An AGU Joint Special Collection

Wintertime Airborne Measurements of Ice Nucleating Particles in the High Arctic: A Hint to a Marine, Biogenic Source for Ice Nucleating Particles

M. Hartmann[1], K. Adachi[2], O. Eppers[3,4], C. Haas[5], A. Herber[6], R. Holzinger[7], A. Hünerbein[8], E. Jäkel[9], C. Jentzsch[1], M. van Pinxteren[10], H. Wex[1], S. Willmes[11], and F. Stratmann[1]

[1]Experimental Aerosol and Cloud Microphysics, Leibniz Institute for Tropospheric Research, Leipzig, Germany, [2]Department of Atmosphere, Ocean and Earth System Modeling Research, Meteorological Research Institute, Tsukuba, Japan, [3]Particle Chemistry, Max Planck Institute for Chemistry, Mainz, Germany, [4]Institute for Atmospheric Physics, Johannes Gutenberg University of Mainz, Mainz, Germany, [5]Sea Ice Physics, Alfred Wegener Institute, Bremerhaven, Germany, [6]Polar Meteorology, Alfred Wegener Institute, Bremerhaven, Germany, [7]Institute for Marine and Atmospheric Research, Utrecht University, Utrecht, Netherlands, [8]Remote Sensing of Atmospheric Processes, Leibniz Institute for Tropospheric Research, Leipzig, Germany, [9]Institute for Meteorology, Leipzig University, Leipzig, Germany, [10]Atmospheric Chemistry Department, Leibniz Institute for Tropospheric Research, Leipzig, Germany, [11]Environmental Meteorology, Trier University, Trier, Germany

Key Points:
- Ice nucleating particles on airborne filter samples containing mainly Arctic marine boundary layer aerosol initiate freezing at −7.5°C
- At −15°C, concentrations of ice nucleating particles ranged from up to $2 \cdot 10^{-2}$ L^{-1} down to below 10^{-3} L^{-1}
- A local marine source and biogenic origin for the high-temperature ice nucleating particles is likely

Supporting Information:
- Supporting Information S1

Correspondence to:
M. Hartmann,
markus.hartmann@tropos.de

Citation:
Hartmann, M., Adachi, K., Eppers, O., Haas, C., Herber, A., Holzinger, R., et al. (2020). Wintertime airborne measurements of ice nucleating particles in the high Arctic: A hint to a marine, biogenic source for ice nucleating particles. *Geophysical Research Letters*, *47*, e2020GL087770. https://doi.org/10.1029/2020GL087770

Received 10 MAR 2020
Accepted 27 MAY 2020
Accepted article online 9 JUN 2020

Abstract Ice nucleating particles (INPs) affect the radiative properties of cold clouds. Knowledge concerning their concentration above ground level and their potential sources is scarce. Here we present the first highly temperature resolved ice nucleation spectra of airborne samples from an aircraft campaign during late winter in 2018. Most INP spectra featured low concentration levels ($<3 \cdot 10^{-4}$ L^{-1} at −15°C). However, we also found INP concentrations of up to $1.8 \cdot 10^{-2}$ L^{-1} at −15°C and freezing onsets as high as −7.5°C for samples mainly from the marine boundary layer. Shape and onset temperature of the ice nucleation spectra of those samples as well as heat sensitivity hint at biogenic INP. Colocated measurements additionally indicate a local marine influence rather than long-range transport. Our results suggest that even in late winter above 80°N a local marine source for biogenic INP, which can efficiently nucleate ice at high temperatures, is present.

Plain Language Summary Clouds are a key factor in the energy budget of the Arctic atmosphere. Ice nucleating particles (INPs) can modify the radiation properties and lifetime of clouds by affecting the relative abundance of liquid and frozen droplets in a cloud. Despite this important ability, knowledge about the INP concentration above ground level is limited as airborne INP measurements are very scarce in the Arctic. Here we present results from an aircraft campaign, which took place during the late winter of 2018 in latitudes above 80°N. We found INP concentrations at above −15°C, which are similar to those found in midlatitudes. These INPs also initiate freezing already at high temperatures. We found indications that the INPs are biogenic and originate from a local, marine source, rather than being transported from midlatitudes into the Arctic. Due to the presence of numerous cracks, open leads and polynyas in the sea ice in the investigation area, the ocean may provide a source for these biogenic INP in an environment, where sources on land are still shrouded in snow and ice. However, in a warming Arctic contributions from different sources might change, making the characterization of the current state important.

1. Introduction

No other region on the Earth is affected more severely by global warming than the Arctic, a phenomenon which is typically referred to as Arctic amplification. The interaction, strength, and relative importance of the processes relevant for Arctic amplification are not yet fully understood, and hence, models fail to reproduce and predict the changes in the Arctic (Pithan & Mauritsen, 2014; Serreze & Barry, 2011).

Clouds play a significant role in the global climate system and are especially important for the energy budget of the Arctic boundary layer (Intrieri, 2002; IPCC, 2014). They can have a cooling effect by reflecting shortwave solar radiation or lead to a warming effect if they reflect terrestrial longwave radiation. The net

radiative effect of a cloud depends on various parameters, for example, altitude, size, thickness, the relative abundance of liquid and frozen water, and season (Intrieri, 2002; Shupe & Intrieri, 2004; Turner et al., 2018). In the Arctic, where the underlying ground has a high albedo, the net cloud radiative effect results in warming, enhancing the melting of snow and sea ice (Stramler et al., 2011; Vavrus et al., 2011). Despite their importance, clouds and their properties are still not well represented in larger-scale atmospheric models, ultimately leading to radiation biases (English et al., 2014, 2015; Tjernström et al., 2008). Uncertainties are, for example, associated with cloud properties in the Arctic and the influences of cloud condensation nuclei (CCN) and ice nucleating particles (INP) on these properties. CCN and INP control the phase of the cloud, that is, the amount of liquid droplets and ice crystals and hence the optical properties, lifetime and the ability to precipitate the cloud. Perturbations of CCN and INP have an especially huge impact on mixed phase clouds. Loewe et al. (2017), Ovchinnikov et al. (2014), Prenni, DeMott, Kreidenweis, et al. (2007), and Shupe and Intrieri (2004) showed that liquid-only clouds have a 3 times stronger longwave radiative effect than pure ice clouds in the Arctic. Also, the impact of changes in INP is thought to dominate over those in CCN on the cloud phase partitioning (Solomon et al., 2018). Cloud temperatures in March and April vary between −11°C and −19°C (Shupe et al., 2006), therefore INP which initiate primary ice formation at higher temperatures are expected to have the greatest influence on cloud phase.

Local sources of aerosol particles in the Arctic are limited, even more in the winter season than in summer. Open water surfaces within the pack ice are of particular importance as source for aerosol particles in a region lacking other sources. It is known that particle generation exists in open leads independent of wind (Held et al., 2011; Norris et al., 2011). This provides a mechanism for the transfer of material from the sea into the Arctic atmosphere. Numerous studies suggest that biological material from the sea surface microlayer (SML) can act as a highly ice active INP (Alpert et al., 2011a, 2011b; Bigg, 1996, 2011a; Bigg & Leck, 2008; Irish et al., 2017; Knopf et al., 2011; Leck & Bigg, 2005; Schnell & Vali, 1976; Wilson et al., 2015; Zeppenfeld et al., 2019). Microorganisms and their resting spores are also found within and below the sea ice (Rózańska et al., 2008) and blooms of ice algae at the ice water interface, probably initiated by light (Werner et al., 2007), can occur (Cota et al., 1991). Therefore, the open water surfaces within the pack ice can be seen as potential source for biogenic INP. The recent publication by Kirpes et al. (2019) supports this further. They name locally produced sea spray aerosol from open leads the dominant aerosol source in winter. The investigated sea spray aerosol particles featured thick organic coatings, consisting of marine saccharides, amino acids, fatty acids, and divalent cations which are known from exopolymeric secretions produced by sea ice algae and bacteria. Some of these substances were also found in the aforementioned highly ice active SML, suggesting that open leads may also be a source fro INP.

Despite the fact that airborne biogenic material is known to nucleate ice (Burrows et al., 2009; Hara et al., 2015; Lu et al., 2016; Moffett, 2015; Moffett et al., 2015; Mortazavi et al., 2015; Šantl-Temkiv et al., 2015, 2019; Smets et al., 2016), abundance and origin of atmospheric INP over the Arctic Ocean is still not well known due to a scarcity of data. Especially, studies of airborne INP measurements near cloud level are still rare, and the origin of INP remains unclear over ice covered regions like the central Arctic Ocean.

It is evident that the sources and activity of Arctic INPs are not well understood. However, to estimate the radiative properties of Arctic clouds in the future, understanding INP as the base for their cloud-phase-driven optical properties, is important.

2. Methods

2.1. Project Overview and Ice Conditions

The PAMARCMiP 2018 campaign (Polar Airborne Measurements and Arctic Regional Climate Model Simulation Project 2018) combined ground-based and airborne measurements at and in the vicinity of the Villum Research Station (81°36′N, 16°40′W; Greenland). The present study focuses on airborne INP. The respective activities were carried out with the research aircraft Polar 5 (Wesche et al., 2016) from 23 March 2018 to 4 April 2018. A total of 14 research flights were performed during the campaign with the main area of operation being above the sea ice in the Arctic ocean and the Fram Strait. For the master flight tracks refer to Herber (2018).

The campaign coincided with the existence of an unusual, large, refrozen polynya along the northeast coast of Greenland north of Station Nord, over which several flights were performed. This polynya opened in late February 2018, and closed by refreezing and convergence in the weeks after (Ludwig et al., 2019). At the time of the campaign the one month old ice in the refrozen polynya already had a modal and mean thickness of 0.9 m and 2 m respectively resulting from thermodynamic and dynamic growth (Ludwig et al., 2019). However, due to the relatively thin ice and dynamic ice conditions there were many open and refrozen leads.

2.2. INP Sampling and Measurement

Filter sampling of aerosol particles combined with off-line analysis of the collected filter samples were applied for determining the temperature-dependent number concentrations (N_{INP}) of atmospheric INP. The filter samples were collected on board the Polar 5 aircraft with a prototype of the High Volume Aerosol Sampler (HERA). HERA is a self-developed automated filter sampler, which has been specifically designed for aircraft operations. PAMARCMiP was the first deployment of HERA. Aerosol particles were sampled into the aircraft through the shrouded inlet diffuser (diameter 0.35 cm at intake point) as described in Leaitch et al. (2010, 2016). The aspiration of the sample air was almost isokinetic ($U_0/U = 1.04$). The inlet was connected to HERA by an ≈6 m long, horizontal stainless steel tube. Within HERA, the aerosol particles were collected on polycarbonate pore filters (0.2 μm pore size; 47 mm diameter; Nuclepore, Whatman) with a constant sample air flow of around 10 L min^{-1} at ambient temperature and pressure conditions. Since low-particle concentrations were expected, sampling took place during the whole flight without sampling during taxiing, take-off, and landing. The respective sample collection times ranged from 3.5 to 7.2 hr, resulting in sampled air volumes between 2,076 and 4,347 L. Each of the individual filter samples was accompanied by a blank sample, which was treated in the same manner as the samples including the time spent inside HERA (without air flow through the filter). Due to operational reasons only during 12 of the 14 flights filters were sampled, and two times, two consecutive flights were sampled onto the same filter (for more details refer to Table S1 in the supporting information). Flight no. 1 was aborted after only 30 min of sampling; therefore, this samples was excluded from the investigations. All samples were removed from the sampler and stored at −20°C immediately after the flight and kept frozen during the transport until analysis at the Leibniz Institute for Tropospheric Research (TROPOS).

The samples and blank samples were analyzed using the freezing array INDA, which is based on the design ofHill et al. (2016) and described in Chen et al. (2018) and Hartmann et al. (2019). The determination of the ambient N_{INP} in the immersion freezing mode as a function of temperature T is based on Vali (1971). In order to make samples and blank samples comparable, the blank samples were normalized with the same air volume as the corresponding sample, though naturally no air was sucked through the blind samples. In addition, the samples were tested for heat-labile material by measuring the sample material before and after heating (95°C for 60 min). More details on the INDA device are given in the supporting information.

2.3. Colocated Measurements

2.3.1. Transmission Electron Microscopy

Compositions and shapes of individual aerosol particles were measured using transmission electron microscopy (TEM; JEM-1400, JEOL, Tokyo, Japan) with energy dispersive X-ray spectrometer (EDS; X-max 80 mm, Oxford Instruments, Tokyo, Japan). Aerosol particles with ∼0.1–0.7 μm aerodynamic diameter (50% cutoff diameter) were collected on TEM grids with formvar carbon substrate using an impactor sampler (AWS-16, Arios, Tokyo, Japan) with 19 min of sampling time. We either used three or four samples (depending on availability) from flights in 25–27, 30, and 31 March and 4 April (totally 19 samples). In each flight, we analyzed more than 200 particles per grid from randomly selected areas, resulting in measurements of 5,228 particles in total. Particles were classified into dust (particles containing both Fe and Al), sea salt (particles containing both Na and Mg), sulfate (particles containing S), and others based on their compositions. Dust particles were further classified into (mineral) dust, Fe-bearing particles, and fly ash based on their composition and shapes using the same criteria as Moteki et al. (2017). In this study, Fe-bearing particles and fly ash particles were categorized into "other" so that "dust" are only mineral dust particles. Sulfate particles that could be classified in more than two categories (e.g., sodium sulfate) were categorized in nonsulfate categories.

2.3.2. Sea Ice and Lead Fraction

The sea ice fraction and the subtype classification is based on images taken by a commercial digital camera (Jäkel et al., 2019). To document the ice fraction over a large area, the camera was equipped with a 180° fisheye lens with a spatial resolution of 3,908 × 2,600 pixels. The camera was geometrically calibrated in the laboratory. The images taken every 6 s were filtered for cloud-free situations below the aircraft. The method of image classification into thick and thin ice, as well as open water relies on manually selecting red, green, and blue (RGB) thresholds, derived from training samples. For flight tracks which were not observed by the fisheye camera due to instrumental failures, images were extracted from video camera data and classified on a similar approach.

Flights on 30 and 31 March were carried out in combination with electromagnetic (EM) ice thickness measurements (Haas et al., 2010). From the ice thickness measurements it was possible to extract the occurrence and widths of leads along the flight tracks (see supporting information). The ice thickness surveys were also special as they required low flying at altitudes of ≈70 m, enabling air sampling at such low levels.

3. Results and Discussion

Cumulative spectra of N_{INP} versus temperature for all samples and their corresponding field blanks are shown in Figure 1. Three samples (25, 30, and 31 March; green, brown and orange, respectively in Figure 1) show clearly elevated concentrations above −15°C in comparison to the corresponding blanks, and are hereafter referred to as high INP samples. In the following we will mainly focus on these samples. For the remaining ones (gray symbols in Figure 1) the measured concentrations are close to those determined for the field blanks. For these samples, the given values represent upper limits for the prevailing INP concentrations.

N_{INP} at −15°C were $1.8{\cdot}10^{-2}$ L^{-1} (25 March), $4.75{\cdot}10^{-3}$ L^{-1} (30 March), and $6.95{\cdot}10^{-3}$ L^{-1} (31 March). These concentrations are well within the wide range of N_{INP} given by Petters and Wright (2015) in midlatitudes (gray-shaded area in Figure 1). Compared to the few earlier studies of airborne N_{INP} in the Arctic (Borys, 1989; Flyger et al., 1973, 1976; Rogers et al., 2001; Prenni, Petters, Kreidenweis, Demont, et al., 2007), the values we report here were often lower (a factor of 50 at −15°C). However, it should be noted that none of the other airborne studies took place at such high latitudes and as early in the year as PAMARCMiP. The study by Borys (1989) is the most comparable to our own in terms of location and time of the year and also reports the most similar N_{INP}: $1.5{\cdot}10^{-2}$ L^{-1} and 0.46 L^{-1} at −15°C and −25°C, respectively, measured in April in latitudes up to 77°N.

Concerning potential contamination of the samples with combustion aerosol particles produced by the aircraft itself it can be noted that previous aircraft-based INP studies (Rogers et al., 2001), ship-based INP measurements (McCluskey et al., 2018; Thomson et al., 2018), or laboratory investigations (Diehl & Mitra, 1998; Schill et al., 2016) either find no influence of exhaust at all, or find the particles to be only ice active in the cirrus cloud temperature regime. Additionally, the trace gas (CO and CO_2) and the Proton-transfer-reaction mass spectrometry (PTR-MS; benzene and toluene) measurements onboard the Polar 5 do not point toward a contamination with exhaust particles on the high INP days. The low levels of CO and CO_2 (CO lower than 155 ppbv and CO_2 lower than 416.7 ppmv for most of the flight time) also make long-range transport from midlatitudes unlikely on those days. The low levels of acetonitrile throughout the campaign (<100 pmol/mol) can especially exclude significant contamination from biomass burning.

The shapes of the ice nucleation spectra of the three high INP samples, that is, steep slopes followed by plateau regions, are indicative for distinct INP populations close to their source. This is in line with current literature, which also tends to see local sources as the main contributor to N_{INP} above −25°C in the Arctic (Bigg & Leck, 2001; Creamean et al., 2018; Šantl-Temkiv et al., 2019; Tobo et al., 2019; Wex et al., 2019). These studies attribute high ice activity to the presence of biogenic INP. The shape and onset temperature of the ice nucleation spectra of the high INP samples from our study are also hinting at biological INP (Beydoun et al., 2017; O'Sullivan et al., 2018; Welti et al., 2018). The heat treatment of our samples lead to a reduction of ice activity of around 6 K at $f_{ice} = 0.1$ (see supporting information for more details). This confirms the presence of heat-labile INP, which suggests a biogenic nature.

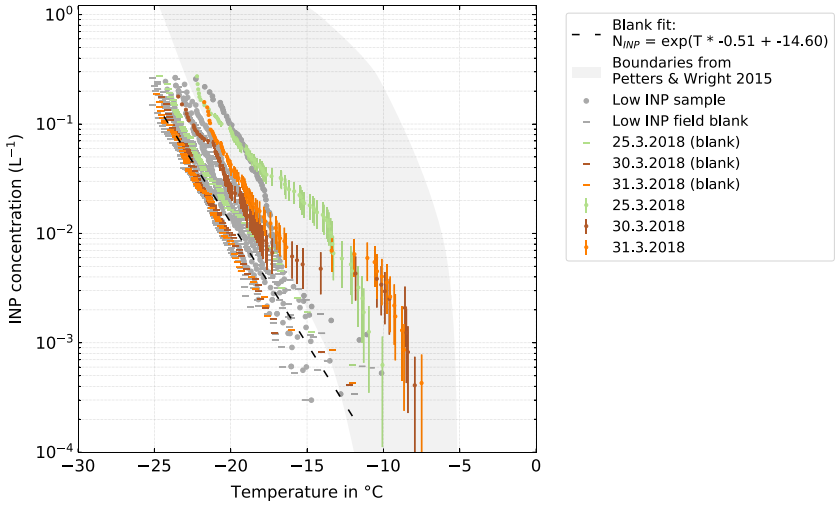

Figure 1. Atmospheric INP concentrations, N_{INP}, of all samples (dot symbols) and corresponding field blanks (minus symbols) collected onboard the Polar 5 aircraft. The samples which are clearly different from their corresponding field blank are colored, while all others are gray. The gray-shaded area is the range of observed N_{INP} by Petters and Wright (2015). The 95% confidence intervals were derived using the formula of Agresti and Coull (1998). For visibility reasons only the confidence intervals for the three high INP samples are shown.

The samples from 30 and 31 March are very similar in terms of their overall shape, freezing onset, and location of the plateau region, while their main difference lies in the absolute concentration of INP. This is a clear indication that the sampled INP populations are the same or at least very similar on both days. The sample from Mar 25 differs from the other two high INP samples featuring a lower freezing onset (−10.1°C on 25 March; −7.9°C on 30 March; −7.5°C on 31 March), a not so pronounced plateau region, and a secondsteep increase in N_{INP}, which follows shortly after the plateau. This is indicative of, compared to the other two samples, different INP being present.

In the following we explore and constrain the origin(s) of the INP on the three high INP days.

The hybrid single-particle Lagrangian integrated trajectory (HYSPLIT) model with GDAS1 meteorological fields was used to calculate back trajectories of the air masses that were sampled along the flight track (Rolph et al., 2017; Stein et al., 2015). Ten-day back trajectories were calculated for each track. Since aircraft measurements cover wide ranges of longitudes, latitudes, and altitudes, a single back trajectory would not represent a sample adequately. Therefore, we calculated multiple back trajectories per flight and sample. The starting points of the trajectories were equally distributed along the flight track. For the three high INP samples, Figure 2 shows the back trajectories (3, 5, and 10 days back; circles with a bluish tone fading with age) and the flight track (black line) on top of the AMSR2 sea ice concentration (Spreen et al., 2008) of the respective day.

Since the spatial uncertainty of the back trajectories grows rapidly over time (Engström & Magnusson, 2009; Harris et al., 2005; Kahl, 1993), the 10-day back trajectories are presented only for completeness, while the further evaluation is based on the 5-day back trajectories. The back trajectories for the other flights can be found in the supporting information. On 25 March most of the back trajectories end in the Chukchi Sea and run over the East Siberian Sea and Laptev Sea and then along the 85° meridian straight to the aircraft. On 30 March the trajectories end in the Beaufort Sea and travel in parallel to the Northern coast of Canada to the Polar 5 aircraft. The East Siberian Sea is the end region for the back trajectories on 31 March, from there they run across the North Pole straight to the aircraft. In general, the pathway of the back trajectories is quite uniform for the individual flights on 25, 30, and 31 March. However, except for the fact that they run almost exclusively over ice-covered sea and not over land, trajectories of the three samples differ considerably. When also the height profile of the trajectories is considered, it can be seen that on 30 and 31 March most back trajectories start and reside for the majority of their travel time at altitudes of a few 100 m or below. Low back trajectories can also be found on 25 March, but not as low and frequent as on the other two high INP days.

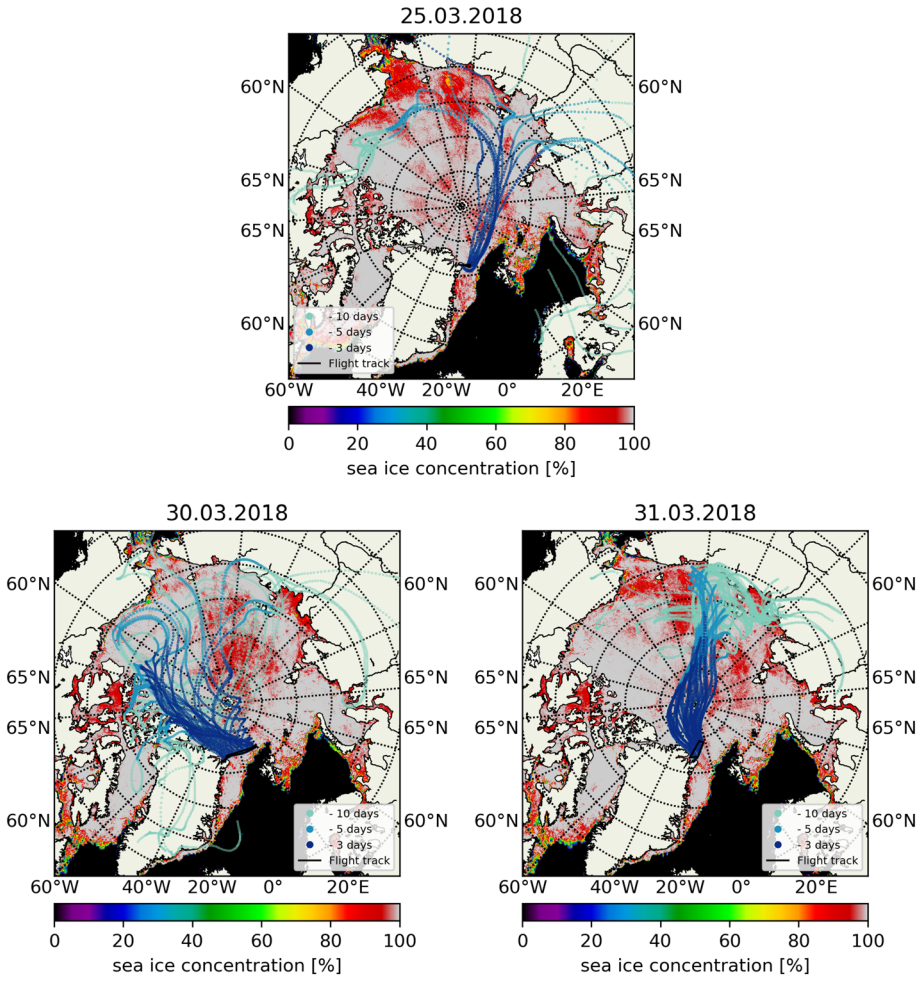

Figure 2. HYSPLIT back trajectories (3, 5, and 10 days back; circles with a bluish tone fading with age) along the flight track (black line) and the underlying AMSR2 sea ice concentration (Spreen et al., 2008) for every day with a high INP sample.

The temperatures along the back-trajectories on the days with high INPs were compared to those of the low INP days (see Figures S28 and S29 in the SI) to identify a possible difference between these two groups. The idea is that in an air mass with a certain temperature ($T_{airmass}$), the chance is increased that INP, which are ice active at temperatures above $T_{airmass}$ are activated and removed from the atmosphere during transport. Thus, the air mass may contain primarily INP which can only nucleate ice at temperatures below $T_{airmass}$, when it reaches our collection site. However, we found that for the high INP as well as the low INP days, the majority of the air masses mostly featured a temperature of -23°C, which is far below the temperature at which we observed the increased INP concentrations on the high INP days (-15°C and above). Therefore, differences in $T_{airmass}$ can not explain the different INP concentrations. We consider this a further indication that the highly ice active biogenic INP we observed originate from a regional source rather than long-range transport.

Figure 3 reveals that the flights on the high INP days are characterized by very low flight altitudes for extended amounts of time (a table with the flight characteristics can be found in the supporting information). Especially, 30 and 31 March feature very low average altitudes, since the aircraft alternated between legs at 70 and 170 m for most of the flight because of the sea ice thickness measurements performed on these days.

Figure 4 shows normalized histograms of the fraction of thin ice determined from the surface type classification based on images of the surface taken directly beneath the aircraft for the high INP days. This shows that high fractions of thin ice were primarily present on the days when high INP concentrations were observed.

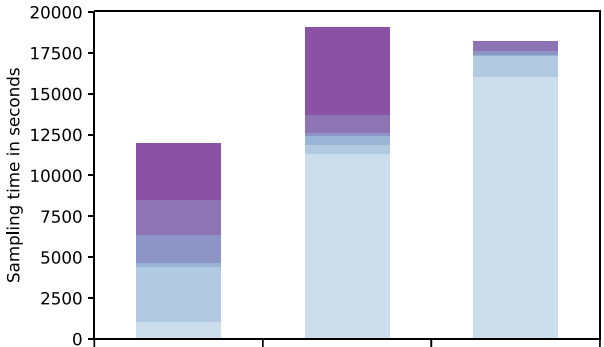

	Mar 25	Mar 30	Mar 31
<5000 m	100.0%	100.0%	100.0%
<2000 m	71.0%	72.0%	100.0%
<1000 m	53.4%	66.2%	96.7%
<500 m	38.6%	64.9%	95.4%
<300 m	36.6%	62.1%	95.1%
<200 m	8.6%	59.6%	88.4%

Figure 3. Stacked bar plot of the sampling time in different height intervals. The corresponding table shows the percentage of sampling time for which sampling took place below a certain height.

Due to the low temperatures, the thin ice was most likely newly formed, rather than by thawing of thicker ice. Therefore it is probable the surfaces covered by thin ice are refrozen leads that were open water surfaces shortly before. The sea ice thickness flights on 30 and 31 March corroborate this by showing the presence of up to several hundred meter long leads, where the sea ice thickness is below the accuracy of the measurement (see the supporting information). This confirms that on all high INP days open water surfaces as potential source for INP were directly beneath the flight path of the aircraft.

Open leads can act as a weak source for particles, which may become important when other more dominant sources are not present. Also, Rogers et al. (2001) hypothesized about a biological INP source from open leads in close proximity, when they observed high INP concentrations at low altitudes (~100 m) over pack ice. Recently, INP collected in the Arctic during summer were also connected to a marine source, a phytoplankton bloom in this case, by Creamean et al. (2019). Impactor samples which were also collected onboard the Polar 5 aircraft and subsequently analyzed with TEM, contain high fractions of sea salt, which is a clear indicator for a marine influence. Dust is also present on samples from all high INP days, but at much lower concentrations compared to sea salt. In Table S1 in the supporting information, flight and sample metrics, as well as results from TEM analysis are compiled for every sample.

For two probed filters (301 March and 2 April) aliphatic amines could be measured. The measurement is limited to these samples as performing the analysis prevented the conduction of the test for heat-labile INP. Aliphatic amines were detected in (blank-corrected) concentrations of $15 \pm 1.2\,\mathrm{ng\,m^{-3}}$ (sum of dimethyl amine and diethyl amine). Amines in the atmosphere can have various origins, however, their presence in remote marine locations has been attributed to local marine, biogenic sources (Ge et al., 2011). As dissolved gaseous compounds, they are released to the atmosphere and form or condense on aerosol particles. Therefore, the presence of particulate amines is not necessarily connected to INP that are potentially transferred to the atmosphere during bubble bursting processes. However, the presence of aliphatic amines in the Arctic in concentrations that are about 3 times higher compared to, for example, ground-based aerosol particle amine concentrations in the tropical Atlantic Ocean (van Pinxteren et al., 2019) suggests the presence of biological activity within the Arctic Ocean in late winter.

Satellite remote sensing products can provide insight on the underlying surface beneath the flight tracks and back trajectories. The AMSR2 sea ice concentration data (Spreen et al., 2008) and the ArcLeads maps of open leads (Willmes & Heinemann, 2015, 2016) show that throughout the whole investigation area large-scale cracks in the sea ice are present (Figure 2 and supporting information). The sea ice in the region east of Villum in the Fram Strait displays a higher degree of fragmentation compared to the region north of Villum. The ArcLeads maps also reveal one of the prominent Arctic polynya, the Northeast Water polynya (≈81°N, 13°W, Preußer et al., 2016), opening up and growing in size, especially since 20 March. It should be noted that the aircraft was never closer to the polynya for longer than on 25 March.

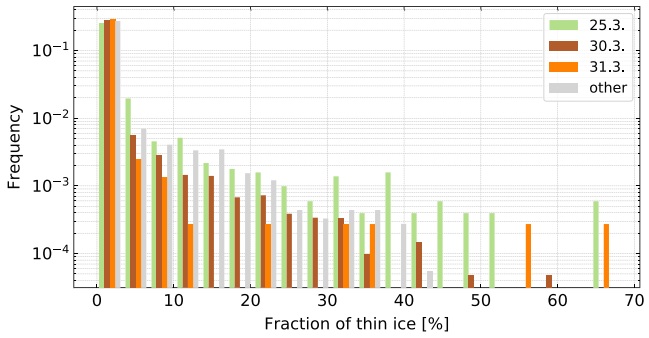

Figure 4. Histogram of the the fraction of thin ice for the flights with high INP concentrations and the other flights with available sea ice fraction measurements (Flight 3 on 26 March; Flights 6 and 7 on 28 March). Histograms are normalized.

However, the existence of open water surfaces is only a sufficient condition for the observation of high N_{INP}, not a necessary or necessary and sufficient condition. Therefore, we do not observe increased N_{INP} on all 12 samples despite the fact, that open leads are present to some degree on every day. Another point has to be stressed: The source strength for INP in the Arctic is still unknown, as the sources themselves are still in discussion. The discussed sources are likely to vary a lot and the same applies to the known sources of INP in other regions (Creamean et al., 2019; Welti et al., 2018).

Overall, the presented chain of thought is as follows: For high N_{INP} on some flights, no common air mass origin was indicated by back trajectories; on these days, samples were taken at exceptional low flight altitude, numerous open leads directly beneath and in the surroundings of the flight track and sea salt is present in collected aerosol samples. This is highly suggestive for a local marine source of high temperature biogenic INP in the Arctic, above 80°N, during late winter.

4. Summary and Conclusion

The INP measurements made during PAMARCMiP provide the first continuous ice nucleation spectra of airborne INP in the Arctic. They also add valuable data to the the very small pool of airborne INP measurements especially in late winter/early spring. On 3 of 12 samples we found INP concentrations above those of the field blanks. N_{INP} above −15°C were comparable to measurements in midlatitudes (Petters & Wright, 2015) and to Arctic airborne measurements, which were taken at similar latitude and season (Borys, 1989). Shape (steepness) and onset temperature of the freezing spectra for those days as well as the heat sensitivity hint at biogenic INP from a local source. Trace gas and PTR-MS measurements show that long-range transport and influence by the aircraft exhaust is unlikely. The flights during which the high INP samples were taken feature low flight altitudes for extended amounts of time. TEM analysis of collocated impactor samples supports a marine influence for those flights. Due to the presence of numerous cracks, open leads, and polynyas in the sea ice of the investigation area, the ocean may provide a source for biogenic particles in an environment, where terrestrial sources are still shrouded in snow and ice. Our results therefore suggest the presence of a local marine source for high-temperature biogenic INP in the Arctic, above 80°, during late winter.

Data Availability Statement

Freezing spectra reported in the manuscript are available at this site (https://doi.pangaea.de/10.1594/PANGAEA.899635).

Acknowledgments
We gratefully acknowledge the funding by the Deutsche Forschungsgemeinschaft (DFG, German Research Foundation)-Projektnummer 268020496-TRR 172, within the Transregional Collaborative Research Center "ArctiC Amplification: Climate Relevant Atmospheric and SurfaCe Processes, and Feedback Mechanisms (AC)^3". K. A. acknowledges the support by the Environment Research and Technology Development Fund (2-1703) of Environmental Restoration and Conservation Agency.

References

Agresti, A., & Coull, B. A. (1998). Approximate is better than "exact" for interval estimation of binomial proportions. *The American Statistician*, *52*(2), 119–126. https://doi.org/10.1080/00031305.1998.10480550

Alpert, P. A., Aller, J. Y., & Knopf, D. A. (2011a). Ice nucleation from aqueous NaCl droplets with and without marine diatoms. *Atmospheric Chemistry and Physics*, *11*(12), 5539–5555. https://doi.org/10.5194/acp-11-5539-2011

Alpert, P. A., Aller, J. Y., & Knopf, D. A. (2011b). Initiation of the ice phase by marine biogenic surfaces in supersaturated gas and supercooled aqueous phases. *Physical Chemistry Chemical Physics*, *13*(44), 19,882–19,894. https://doi.org/10.1039/c1cp21844a

Beydoun, H., Polen, M., & Sullivan, R. C. (2017). A new multicomponent heterogeneous ice nucleation model and its application to Snomax bacterial particles and a Snoma-illite mineral particle mixture. *Atmospheric Chemistry and Physics*, *17*(22), 13,545–13,557. https://doi.org/10.5194/acp-17-13545-2017

Bigg, E. K. (1996). Ice forming nuclei in the high Arctic. *Tellus B*, *48*(2), 223–233. https://doi.org/10.1034/j.1600-0889.1996.t01-1-00007.x

Bigg, E. K., & Leck, C. (2001). Properties of the aerosol over the central Arctic Ocean. *Journal of Geophysical Research*, *106*(D23), 32,101–32,109. https://doi.org/10.1029/1999JD901136

Bigg, E. K., & Leck, C. (2008). The composition of fragments of bubbles bursting at the ocean surface. *Journal of Geophysical Research*, *113*, D11209. https://doi.org/10.1029/2007JD009078

Borys, R. D. (1989). Studies of ice nucleation by Arctic aerosol on AGASP-II. *Journal of Atmospheric Chemistry*, *9*(1-3), 169–185. https://doi.org/10.1007/BF00052831

Burrows, S. M., Elbert, W., Lawrence, M. G., & Pöschl, U. (2009). Bacteria in the global atmosphere—Part 1: Review and synthesis of literature data for different ecosystems. *Atmospheric Chemistry and Physics*, *9*(23), 9263–9280. https://doi.org/10.5194/acp-9-9263-2009

Chen, J., Wu, Z., Augustin-Bauditz, S., Grawe, S., Hartmann, M., Pei, X., & Wex, H. (2018). Ice-nucleating particle concentrations unaffected by urban air pollution in Beijing, China. *Atmospheric Chemistry and Physics*, *18*(5), 3523–3539. https://doi.org/10.5194/acp-18-3523-2018

Cota, G., Legendre, L., Gosselin, M., & Ingram, R. (1991). Ecology of bottom ice algae: I. Environmental controls and variability. *Journal of Marine Systems*, *2*(3-4), 257–277. https://doi.org/10.1016/0924-7963(91)90036-T

Creamean, J. M., Cross, J. N., Pickart, R., McRaven, L., Lin, P., Pacini, A., & DeMott, P. J. (2019). Ice nucleating particles carried from below a phytoplankton bloom to the Arctic atmosphere. *Geophysical Research Letters*, *46*, 8572–8581. https://doi.org/10.1029/2019GL083039

Creamean, J. M., Kirpes, R. M., Pratt, K. A., Spada, N. J., Maahn, M., de Boer, G., & China, S. (2018). Marine and terrestrial influences on ice nucleating particles during continuous springtime measurements in an Arctic oilfield location. *Atmospheric Chemistry and Physics*, *18*(24), 18,023–18,042. https://doi.org/10.5194/acp-18-18023-2018

Diehl, K., & Mitra, S. (1998). A laboratory study of the effects of a kerosene-burner exhaust on ice nucleation and the evaporation rate of ice crystals. *Atmospheric Environment*, *32*(18), 3145–3151. https://doi.org/10.1016/S1352-2310(97)00467-6

English, J. M., Gettelman, A., & Henderson, G. R. (2015). Arctic radiative fluxes: Present-day biases and future projections in CMIP5 models. *Journal of Climate*, *28*(15), 6019–6038. https://doi.org/10.1175/JCLI-D-14-00801.1

English, J. M., Kay, J. E., Gettelman, A., Liu, X., Wang, Y., Zhang, Y., & Chepfer, H. (2014). Contributions of clouds, surface albedos, and mixed-phase ice nucleation schemes to Arctic radiation biases in CAM5. *Journal of Climate*, *27*(13), 5174–5197. https://doi.org/10.1175/JCLI-D-13-00608.1

Engström, A., & Magnusson, L. (2009). Estimating trajectory uncertainties due to flow dependent errors in the atmospheric analysis. *Atmospheric Chemistry and Physics*, *9*(22), 8857–8867. https://doi.org/10.5194/acp-9-8857-2009

Flyger, H., Hansen, K., Megaw, W. J., & Cox, L. C. (1973). The background level of the summer tropospheric aerosol over Greenland and the North Atlantic Ocean. *Journal of Applied Meteorology*, *12*(1), 161–174. https://doi.org/10.1175/1520-0450(1973)012<0161:TBLOTS>2.0.CO;2

Flyger, H., Heidam, N., Hansen, K., Megaw, W., Walther, E., & Hogan, A. (1976). The background level of the summer tropospheric aerosol, sulphur dioxide and ozone over Greenland and the North Atlantic Ocean. *Journal of Aerosol Science*, *7*(2), 103–140. https://doi.org/10.1016/0021-8502(76)90069-0

Ge, X., Wexler, A. S., & Clegg, S. L. (2011). Atmospheric amines—Part II. Thermodynamic properties and gas/particle partitioning. *Atmospheric Environment*, *45*(3), 561–577. https://doi.org/10.1016/j.atmosenv.2010.10.013

Haas, C., Hendricks, S., Eicken, H., & Herber, A. (2010). Synoptic airborne thickness surveys reveal state of Arctic sea ice cover. *Geophysical Research Letters*, *37*, L09501. https://doi.org/10.1029/2010GL042652

Hara, K., Zhang, D., Matsusaki, H., Sadanaga, Y., Ikeda, K., Hanaoka, S., & Hatakeyama, S. (2015). UV-tolerant culturable bacteria in an Asian dust plume transported over the east China Sea. *Aerosol and Air Quality Research*, *15*, 591–599. https://doi.org/10.4209/aaqr.2014.03.0067

Harris, J. M., Draxler, R. R., & Oltmans, S. J. (2005). Trajectory model sensitivity to differences in input data and vertical transport method. *Journal of Geophysical Research*, *110*, D14109. https://doi.org/10.1029/2004JD005750

Hartmann, M., Blunier, T., Brügger, S., Schmale, J., Schwikowski, M., Vogel, A., & Stratmann, F. (2019). Variation of ice nucleating particles in the European Arctic over the last centuries. *Geophysical Research Letters*, *46*, 4007–4016. https://doi.org/10.1029/2019GL082311

Held, A., Brooks, I. M., Leck, C., & Tjernström, M. (2011). On the potential contribution of open lead particle emissions to the central Arctic aerosol concentration. *Atmospheric Chemistry and Physics*, *11*(7), 3093–3105. https://doi.org/10.5194/acp-11-3093-2011

Herber, A. (2018). Master tracks in different resolutions during POLAR 5 campaign PAMARCMIP_2018. PANGAEA https://doi.org/10.1594/PANGAEA.890848

Hill, T. C. J., DeMott, P. J., Tobo, Y., Fröhlich-Nowoisky, J., Moffett, B. F., Franc, G. D., & Kreidenweis, S. M. (2016). Sources of organic ice nucleating particles in soils. *Atmospheric Chemistry and Physics*, *16*(11), 7195–7211. https://doi.org/10.5194/acp-16-7195-2016

IPCC (2014). *Climate change 2013—The physical science basis*. Cambridge: Cambridge University Press. (Intergovernmental Panel on Climate Change, Ed.). https://doi.org/10.1017/CBO9781107415324

Intrieri, J. M. (2002). An annual cycle of Arctic surface cloud forcing at SHEBA. *Journal of Geophysical Research*, *107*(C10), 8039. https://doi.org/10.1029/2000JC000439

Irish, V. E., Elizondo, P., Chen, J., Chou, C., Charette, J., Lizotte, M., & Bertram, A. K. (2017). Ice-nucleating particles in Canadian Arctic sea-surface microlayer and bulk seawater. *Atmospheric Chemistry and Physics*, *17*(17), 10,583–10,595. https://doi.org/10.5194/acp-17-10583-2017

Jäkel, E., Stapf, J., Wendisch, M., Nicolaus, M., Dorn, W., & Rinke, A. (2019). Validation of the sea ice surface albedo scheme of the regional climate model HIRHAM–NAOSIM using aircraft measurements during the ACLOUD/PASCAL campaigns. *The Cryosphere*, *13*(6), 1695–1708. https://doi.org/10.5194/tc-13-1695-2019

Kahl, J. D. (1993). A cautionary note on the use of air trajectories in interpreting atmospheric chemistry measurements. *Atmospheric Environment. Part A. General Topics*, *27*(17), 3037–3038. https://doi.org/10.1016/0960-1686(93)90336-W

Kirpes, R. M., Bonanno, D., May, N. W., Fraund, M., Barget, A. J., Moffet, R. C., & Pratt, K. A. (2019). Wintertime Arctic sea spray aerosol composition controlled by sea ice lead microbiology. *ACS Central Science*, *5*(11), 1760–1767. https://doi.org/10.1021/acscentsci.9b00541

Knopf, D. A., Alpert, P. A., Wang, B., & Aller, J. Y. (2011). Stimulation of ice nucleation by marine diatoms. *Nature Geoscience*, *4*(2), 88–90. https://doi.org/10.1038/ngeo1037

Leaitch, W. R., Korolev, A., Aliabadi, A. A., Burkart, J., Willis, M. D., Abbatt, J. P., & Brauner, R. (2016). Effects of 20-100 nm particles on liquid clouds in the clean summertime Arctic. *Atmospheric Chemistry and Physics*, *16*(17), 11,107–11,124. https://doi.org/10.5194/acp-16-11107-2016

Leaitch, W. R., Lohmann, U., Russell, L. M., Garrett, T., Shantz, N. C., Toom-Sauntry, D., & Jayne, J. T. (2010). Cloud albedo increase from carbonaceous aerosol. *Atmospheric Chemistry and Physics*, *10*(16), 7669–7684. https://doi.org/10.5194/acp-10-7669-2010

Leck, C., & Bigg, E. K. (2005). Biogenic particles in the surface microlayer and overlaying atmosphere in the central Arctic Ocean during summer. *Tellus B: Chemical and Physical Meteorology*, *57*(4), 305–316. https://doi.org/10.3402/tellusb.v57i4.16546

Loewe, K., Ekman, A. M., Paukert, M., Sedlar, J., Tjernström, M., & Hoose, C. (2017). Modelling micro- and macrophysical contributors to the dissipation of an Arctic mixed-phase cloud during the Arctic Summer Cloud Ocean Study (ASCOS). *Atmospheric Chemistry and Physics*, *17*(11), 6693–6704. https://doi.org/10.5194/acp-17-6693-2017

Lu, Z., Du, P., Du, R., Liang, Z., Qin, S., Li, Z., & Wang, Y. (2016). The diversity and role of bacterial ice nuclei in rainwater from mountain sites in China. *Aerosol and Air Quality Research*, *16*(3), 640–652. https://doi.org/10.4209/aaqr.2015.05.0315

Ludwig, V., Spreen, G., Haas, C., Istomina, L., Kauker, F., & Murashkin, D. (2019). The 2018 North Greenland polynya observed by a newly introduced merged optical and passive microwave sea-ice concentration dataset. *The Cryosphere*, *13*(7), 2051–2073. https://doi.org/10.5194/tc-13-2051-2019

McCluskey, C. S., Hill, T. C. J., Humphries, R. S., Rauker, A. M., Moreau, S., Strutton, P. G., & DeMott, P. J. (2018). Observations of ice nucleating particles over Southern Ocean waters. *Geophysical Research Letters*, *45*, 11,989–11,997. https://doi.org/10.1029/2018GL079981

Moffett, B. F. (2015). Ice nucleation in mosses and liverworts. *Lindbergia*, *38*, 14–16.

Moffett, B. F., Getti, G., Henderson-Begg, S. K., & Hill, T. C. (2015). Ubiquity of ice nucleation in lichen—Possible atmospheric implications. *Lindbergia*, *38*(November), 39–43.

Mortazavi, R., Attiya, S., & Ariya, P. A. (2015). *Atmospheric Chemistry and Physics*, *15*(11), 6183–6204. https://doi.org/10.5194/acp-15-6183-2015

Moteki, N., Adachi, K., Ohata, S., Yoshida, A., Harigaya, T., Koike, M., & Kondo, Y. (2017). Anthropogenic iron oxide aerosols enhance atmospheric heating. *Nature Communications*, *1*, 15329. https://doi.org/10.1038/ncomms15329

Norris, S. J., Brooks, I. M., de Leeuw, G., Sirevaag, A., Leck, C., Brooks, B. J., & Tjernström, M. (2011). Measurements of bubble size spectra within leads in the Arctic summer pack ice. *Ocean Science*, *7*(1), 129–139. https://doi.org/10.5194/os-7-129-2011

O'Sullivan, D., Adams, M. P., Tarn, M. D., Harrison, A. D., Vergara-Temprado, J., Porter, G. C. E., & Murray, B. J. (2018). Contributions of biogenic material to the atmospheric ice-nucleating particle population in North Western Europe. *Scientific Reports*, *8*(1), 13821. https://doi.org/10.1038/s41598-018-31981-7

Ovchinnikov, M., Ackerman, A. S., Avramov, A., Cheng, A., Fan, J., Fridlind, A. M., & Sulia, K. (2014). Intercomparison of large-eddy simulations of Arctic mixed-phase clouds: Importance of ice size distribution assumptions. *Journal of Advances in Modeling Earth Systems*, *6*, 223–248. https://doi.org/10.1002/2013MS000282

Petters, M. D., & Wright, T. P. (2015). Revisiting ice nucleation from precipitation samples. *Geophysical Research Letters*, *42*, 8758–8766. https://doi.org/10.1002/2015GL065733

Pithan, F., & Mauritsen, T. (2014). Arctic amplification dominated by temperature feedbacks in contemporary climate models. *Nature Geoscience*, *7*(3), 181–184. https://doi.org/10.1038/ngeo2071

Prenni, A. J., DeMott, P. J., Kreidenweis, S. M., Harrington, J. Y., Avramov, A., Verlinde, J., & Olsson, P. Q. (2007). Can ice-nucleating aerosols affect Arctic seasonal climate? *Bulletin of the American Meteorological Society*, *88*(4), 541–550. https://doi.org/10.1175/BAMS-88-4-541

Prenni, A. J., Petters, M. D., Kreidenweis, S. M., DeMott, P. J., & Ziemann, P. J. (2007). Cloud droplet activation of secondary organic aerosol. *Journal of Geophysical Research*, *112*, D10223. https://doi.org/10.1029/2006JD007963

Preußer, A., Heinemann, G., Willmes, S., & Paul, S. (2016). Circumpolar polynya regions and ice production in the Arctic: Results from MODIS thermal infrared imagery from 2002/2003 to 2014/2015 with a regional focus on the Laptev Sea. *The Cryosphere*, *10*(6), 3021–3042.

Rózańska, M., Poulin, M., & Gosselin, M. (2008). Protist entrapment in newly formed sea ice in the Coastal Arctic Ocean. *Journal of Marine Systems*, *74*(3-4), 887–901. https://doi.org/10.1016/j.jmarsys.2007.11.009

Rogers, D. C., DeMott, P. J., & Kreidenweis, S. M. (2001). Airborne measurements of tropospheric ice-nucleating aerosol particles in the Arctic spring. *Journal of Geophysical Research*, *106*(D14), 15,053–15,063. https://doi.org/10.1029/2000JD900790

Rolph, G., Stein, A., & Stunder, B. (2017). Real-time Environmental Applications and Display sYstem: READY. *Environmental Modelling & Software*, *95*, 210–228. https://doi.org/10.1016/j.envsoft.2017.06.025

Šantl-Temkiv, T., Lange, R., Beddows, D. C., Rauter, U., Pilgaard, S., Dall'Osto, M., & Wex, H. (2019). Biogenic sources of ice nucleation particles at the High Arctic Site Villum Research Station. *Environmental Science & Technology*, *53*(18), acs.est.9b00991. https://doi.org/10.1021/acs.est.9b00991

Šantl-Temkiv, T., Sahyoun, M., Finster, K., Hartmann, S., Augustin-Bauditz, S., Stratmann, F., & Karlson, U. G. (2015). Characterization of airborne ice-nucleation-active bacteria and bacterial fragments. *Atmospheric Environment*, *109*, 105–117. https://doi.org/10.1016/j.atmosenv.2015.02.060

Schill, G. P., Jathar, S. H., Kodros, J. K., Levin, E. J. T., Galang, A. M., Friedman, B., & DeMott, P. J. (2016). Ice-nucleating particle emissions from photochemically aged diesel and biodiesel exhaust. *Geophysical Research Letters*, *43*, 5524–5531. https://doi.org/10.1002/2016GL069529

Schnell, R. C., & Vali, G. (1976). Biogenic ice nuclei: Part I. Terrestrial and marine sources. *Journal of the Atmospheric Sciences*, *33*(8), 1554–1564. https://doi.org/10.1175/1520-0469(1976)033<1554:BINPIT>2.0.CO;2

Serreze, M. C., & Barry, R. G. (2011). Processes and impacts of Arctic amplification: A research synthesis. *Global and Planetary Change*, *77*(1-2), 85–96. https://doi.org/10.1016/j.gloplacha.2011.03.004

Shupe, M. D., & Intrieri, J. M. (2004). Cloud radiative forcing of the Arctic surface: The influence of cloud properties, surface albedo, and solar zenith angle. *Journal of Climate*, *17*(3), 616–628. https://doi.org/10.1175/1520-0442(2004)017<0616:CRFOTA>2.0.CO;2

Shupe, M. D., Matrosov, S. Y., & Uttal, T. (2006). Arctic Mixed-Phase Cloud Properties Derived from Surface-Based Sensors at SHEBA. *Journal of the Atmospheric Sciences*, *63*(2), 697–711. https://doi.org/10.1175/jas3659.1

Smets, W., Moretti, S., Denys, S., & Lebeer, S. (2016). Airborne bacteria in the atmosphere: Presence, purpose, and potential. *Atmospheric Environment*, *139*(May), 214–221. https://doi.org/10.1016/j.atmosenv.2016.05.038

Solomon, A., de Boer, G., Creamean, J. M., McComiskey, A., Shupe, M. D., Maahn, M., & Cox, C. (2018). The relative impact of cloud condensation nuclei and ice nucleating particle concentrations on phase partitioning in Arctic mixed-phase stratocumulus clouds. *Atmospheric Chemistry and Physics*, *18*(23), 17,047–17,059. https://doi.org/10.5194/acp-18-17047-2018

Spreen, G., Kaleschke, L., & Heygster, G. (2008). Sea ice remote sensing using AMSR-E 89-GHz channels. *Journal of Geophysical Research*, *113*, C02S03. https://doi.org/10.1029/2005JC003384

Stein, A. F., Draxler, R. R., Rolph, G. D., Stunder, B. J. B., Cohen, M. D., & Ngan, F. (2015). NOAA's HYSPLIT atmospheric transport and dispersion modeling system. *Bulletin of the American Meteorological Society*, *96*(12), 2059–2077. https://doi.org/10.1175/BAMS-D-14-00110.1

Stramler, K., Del Genio, A. D., & Rossow, W. B. (2011). Synoptically driven Arctic winter states. *Journal of Climate*, *24*(6), 1747–1762. https://doi.org/10.1175/2010JCLI3817.1

Thomson, E. S., Weber, D., Bingemer, H. G., Tuomi, J., Ebert, M., & Pettersson, J. B. (2018). Intensification of ice nucleation observed in ocean ship emissions. *Scientific Reports*, *8*(1), 1–9. https://doi.org/10.1038/s41598-018-19297-y

Tjernström, M., Sedlar, J., & Shupe, M. D. (2008). How well do regional climate models reproduce radiation and clouds in the arctic? An evaluation of ARCMIP simulations. *Journal of Applied Meteorology and Climatology*, *47*(9), 2405–2422. https://doi.org/10.1175/2008JAMC1845.1

Tobo, Y., Adachi, K., DeMott, P. J., Hill, T. C. J., Hamilton, D. S., Mahowald, N. M., & Koike, M. (2019). Glacially sourced dust as a potentially significant source of ice nucleating particles. *Nature Geoscience*, *12*, 253–258. https://doi.org/10.1038/s41561-019-0314-x

Turner, D. D., Shupe, M. D., & Zwink, A. B. (2018). Characteristic atmospheric radiative heating rate profiles in Arctic clouds as observed at barrow, Alaska. *Journal of Applied Meteorology and Climatology*, *57*(4), 953–968. https://doi.org/10.1175/JAMC-D-17-0252.1

Vali, G. (1971). Quantitative evaluation of experimental results an the heterogeneous freezing nucleation of supercooled liquids. *Journal of the Atmospheric Sciences*, *28*(3), 402–409. https://doi.org/10.1175/1520-0469(1971)028<0402:QEOERA>2.0.CO;2

van Pinxteren, M., Fomba, K. W., van Pinxteren, D., Triesch, N., Hoffmann, E. H., Cree, C. H., & Herrmann, H. (2019). Aliphatic amines at the Cape Verde Atmospheric Observatory: Abundance, origins and sea-air fluxes. *Atmospheric Environment*, *203*, 183–195. https://doi.org/10.1016/j.atmosenv.2019.02.011

Vavrus, S., Holland, M. M., & Bailey, D. A. (2011). Changes in Arctic clouds during intervals of rapid sea ice loss. *Climate Dynamics*, *36*(7-8), 1475–1489. https://doi.org/10.1007/s00382-010-0816-0

Welti, A., Müller, K., Fleming, Z. L., & Stratmann, F. (2018). Concentration and variability of ice nuclei in the subtropical maritime boundary layer. *Atmospheric Chemistry and Physics*, *18*(8), 5307–5320. https://doi.org/10.5194/acp-18-5307-2018

Werner, I., Ikävalko, J., & Schünemann, H. (2007). Sea-ice algae in Arctic pack ice during late winter. *Polar Biology*, *30*(11), 1493–1504. https://doi.org/10.1007/s00300-007-0310-2

Wesche, C., Steinhage, D., & Nixdorf, U. (2016). Polar aircraft Polar5 and Polar6 operated by the Alfred Wegener Institute. *Journal of large-Scale Research Facilities JLSRF*, *2*, A87. https://doi.org/10.17815/jlsrf-2-153

Wex, H., Huang, L., Zhang, W., Hung, H., Traversi, R., Becagli, S., & Stratmann, F. (2019). Annual variability of ice-nucleating particle concentrations at different Arctic locations. *Atmospheric Chemistry and Physics*, *19*(7), 5293–5311. https://doi.org/10.5194/acp-19-5293-2019

Willmes, S., & Heinemann, G. (2015). Pan-Arctic lead detection from MODIS thermal infrared imagery. *Annals of Glaciology*, *56*(69), 29–37. https://doi.org/10.3189/2015AoG69A615

Willmes, S., & Heinemann, G. (2016). Sea-ice wintertime lead frequencies and regional characteristics in the Arctic, 2003–2015. *Remote Sensing*, *1*, 4. https://doi.org/10.3390/rs8010004

Wilson, T. W., Ladino, L. A., Alpert, P. A., Breckels, M. N., Brooks, I. M., Browse, J., & Murray, B. J. (2015). A marine biogenic source of atmospheric ice-nucleating particles. *Nature*, *525*(7568), 234–238. https://doi.org/10.1038/nature14986

Zeppenfeld, S., van Pinxteren, M., Hartmann, M., Bracher, A., Stratmann, F., & Herrmann, H. (2019). Glucose as a potential chemical marker for ice nucleating activity in Arctic seawater and melt pond samples. *Environmental Science & Technology*, *53*(15), acs.est.9b01469. https://doi.org/10.1021/acs.est.9b01469

References From the Supporting Information

Conen, F., Henne, S., Morris, C. E., & Alewell, C. (2012). Atmospheric ice nucleators active ≥−12°C may be quantified on PM10 filters. *Atmospheric Measurement Techniques*, *5*(2), 321–327. https://doi.org/10.5194/amt-5-321-2012

Haas, C., Lobach, J., Hendricks, S., Rabenstein, L., & Pfaffling, A. (2009). Helicopter-borne measurements of sea ice thickness, using a small and lightweight, digital EM system. *Journal of Applied Geophysics*, *67*(3), 234–241. https://doi.org/10.1016/j.jappgeo.2008.05.005

Maslanik, J., & Stroeve, J. (1999). *Near-real-time DMSP SSMIS daily polar gridded sea ice concentrations, version 1*. Boulder, Colorado USA: NASA National Snow and Ice Data Center Distributed Active Archive Center. [North Polar, 2018]. https://doi.org/10.5067/U8C09DWVX9LM